Journal of Physics D: Applied Physics

PAPER

A flexible and transparent β-Ga_2O_3 solar-blind ultraviolet photodetector on mica

To cite this article: Yanxin Sui *et al* 2020 *J. Phys. D: Appl. Phys.* **53** 504001

IOP Publishing Journal of Physics D: Applied Physics

J. Phys. D: Appl. Phys. **53** (2020) 504001 (9pp) https://doi.org/10.1088/1361-6463/abb1e7

A flexible and transparent β-Ga_2O_3 solar-blind ultraviolet photodetector on mica

Yanxin Sui[2,3], Huili Liang[1,2], Wenxing Huo[2], Yan Wang[1,2] and Zengxia Mei[1,2]

[1] Songshan Lake Materials Laboratory, Dongguan, Guangdong, 523808, People's Republic of China
[2] Beijing National Laboratory for Condensed Matter Physics, Institute of Physics, Chinese Academy of Sciences, Beijing 100190, People's Republic of China
[3] School of Physical Sciences, University of Chinese Academy of Sciences, Beijing 100049, People's Republic of China

E-mail: hlliang@iphy.ac.cn and zxmei@iphy.ac.cn

Received 24 June 2020, revised 17 August 2020
Accepted for publication 24 August 2020
Published 1 October 2020

Abstract

In the present work, we report a flexible transparent β-Ga_2O_3 solar-blind ultraviolet (UV) photodetector (PD) fabricated on a mica substrate. A laminated a-Ga_2O_3/Ga/a-Ga_2O_3 structure is thermally annealed at 1050 °C, forming a β-Ga_2O_3 film incorporating Ga nanospheres. A PD based on this nanocomposite film has a spectrum response peak at 250 nm, an extremely low dark current of 0.6 pA at a 10 V bias, a very high I_{light}/I_{dark} ratio of 3×10^6, and a fast recovery speed of less than 50 ms. Robust flexibility is demonstrated by bending tests and 10 000 cycles of a fatigue test with a radius as small as 8 mm. Compared to a room-temperature-fabricated flexible amorphous Ga_2O_3 (a-Ga_2O_3) PD, the flexible β-Ga_2O_3 PD on mica exhibits improved solar-blind UV photoresponse characteristics. The insertion of a gallium interlayer and treatment by high-temperature post annealing are proposed to contribute to a better stoichiometry and lattice order of the β-Ga_2O_3 thin film, as evidenced by the pronounced Raman peaks related to the $Ga_I(O_I)_2$ and Ga_IO_4 vibration modes in β-phase Ga_2O_3. Our research is believed to provide a simple and practical route to achieving flexible transparent β-Ga_2O_3 solar-blind UV PDs, as well as other devices such as flexible transparent phototransistors and power rectifiers.

Keywords: β-Ga_2O_3, solar-blind ultraviolet photodetector, flexible, mica, high-temperature post annealing

(Some figures may appear in colour only in the online journal)

1. Introduction

III-nitride compounds, $Mg_xZn_{1-x}O$, Ga_2O_3, and diamond are well-known wide bandgap semiconductor materials for solar-blind UV detection [1–6]. Among these, Ga_2O_3 has a ~4.9 eV direct bandgap and a high absorption coefficient, which avoids the complicated bandgap engineering problem and enables Ga_2O_3 to be a promising material [7, 8]. So far, great progress has been made in research into Ga_2O_3 UV photodetectors (PDs) [9–14]. Crystalline-phase Ga_2O_3, β-Ga_2O_3 is predominantly preferred in most cases, due to its high crystallinity and low defect density [5]. However, the high growth temperature (usually > 800 °C) which is essential for the synthesis of β-Ga_2O_3 becomes a major hindrance to its utilization in flexible and transparent sensing devices (typically ≈ 80 °C–150 °C) [15, 16]. On the other hand, most of the flexible Ga_2O_3 PDs are produced on amorphous Ga_2O_3 (a-Ga_2O_3), and show a slow response speed, even to the level of seconds, which is called the persistent photoconductivity (PPC) effect. This is generally ascribed to the

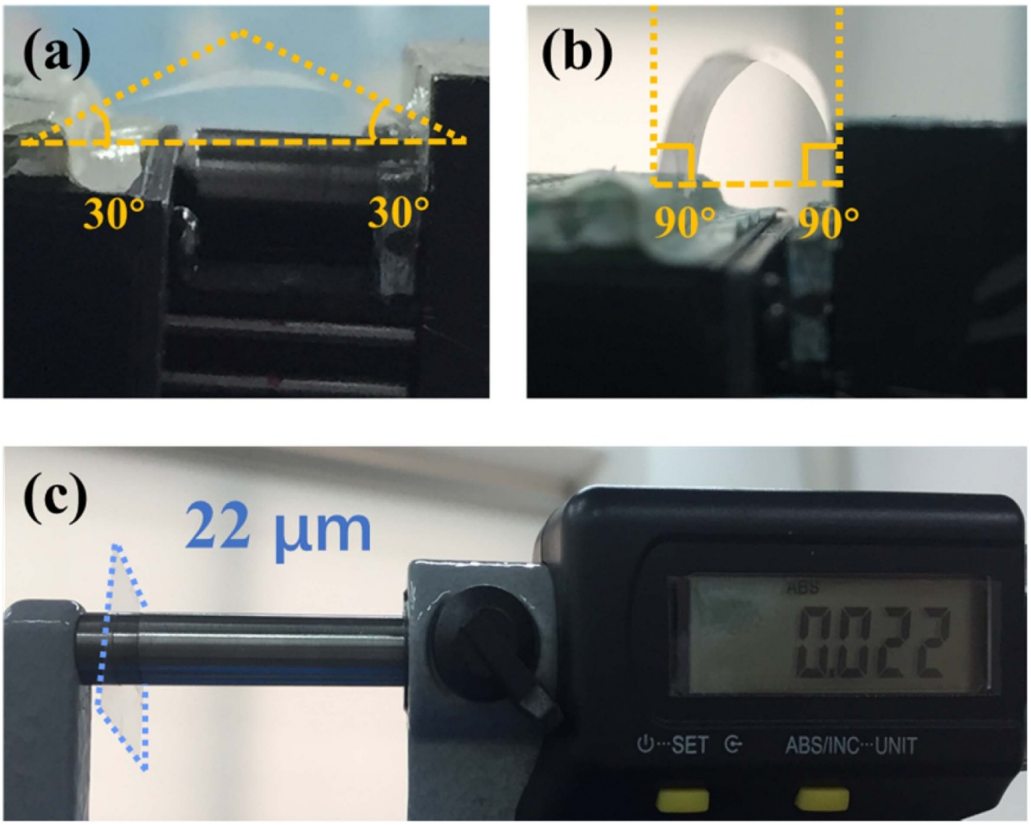

Figure 1. Optical pictures of the 22 μm thick mica substrate.

existence of oxygen vacancy (V_O) defects [17, 18]. A delicate control of oxygen flux in the sputtering process of a-Ga_2O_3 film at room temperature was applied by Cui *et al* to suppress the generation of V_O defects and PPC in flexible Ga_2O_3 UV PDs [9]. Nevertheless, the device manifested an obviously degraded responsivity, by three orders of magnitude, posing an urgent need for a balance between responsivity and response speed. One of the potential approaches to this issue is the fabrication of β-Ga_2O_3 on flexible substrates.

Mica is a well-known kind of layered silicate compound that can be used as an alternative flexible substrate with many outstanding features, such as a high melting point (700 °C–1100 °C), an atomically flat surface, high transparency and compatibility with all deposition and microfabrication techniques [19–22]. Therefore, mica would be an excellent flexible substrate for next-generation flexible transparent electronics, while removing the temperature limitations from the devices' preparation process.

Herein, a fully transparent and flexible β-Ga_2O_3 solar-blind UV PD on mica is reported with a remarkably enhanced I_{light}/I_{dark} ratio and response speed, compared to a room-temperature-fabricated flexible a-Ga_2O_3 single-layered PD. It should be noticed that instead of a single-layer Ga_2O_3 film, a nanocomposite β-Ga_2O_3 film incorporated with Ga nanospheres (NSs) was adopted by post-annealing an a-Ga_2O_3/Ga/a-Ga_2O_3 laminated film at 1050 °C to achieve a decreased defect density and an improved lattice order.

2. Experimental method

2.1. Treatment of the mica substrate

Fluorphlogopite mica substrates (15 mm × 15 mm × 0.5 mm, Tai Yuan Fluorphlogopite Mica Company) were first split with a surgical blade in a culture dish with deionized water where the force between the layers of the mica could easily be overcome, leading to a relatively flat surface. Then, a relatively thin 15 mm × 15 mm piece of mica (usually < 30 μm) was taken out to be further exfoliated by scotch tape in order to get a fresh surface before being loaded into the vacuum chamber.

2.2. Fabrication of the nanocomposite films

The β-Ga_2O_3 nanocomposite films were synthesized by post-annealing the laminated a-Ga_2O_3/Ga/a-Ga_2O_3 samples, which were reported in our previous work. After annealing at 1050 °C, the Ga interlayer formed discrete metal Ga NSs embedded in the β-Ga_2O_3 matrix, which had already been verified through transmission electron microscopy (TEM) characterizations in our previous work [11]. To evaluate the influence of Ga diffusion on the stoichiometry and lattice order of the β-Ga_2O_3 film, four samples were prepared: 1050 °C post-annealed 120 nm Ga_2O_3 without a Ga interlayer on mica (M1) and quartz (Q1), 1050 °C post-annealed laminated a-Ga_2O_3 (60 nm)/Ga (20 nm)/a-Ga_2O_3 (60 nm) nanocomposite films on mica (M2) and quartz (Q2), respectively.

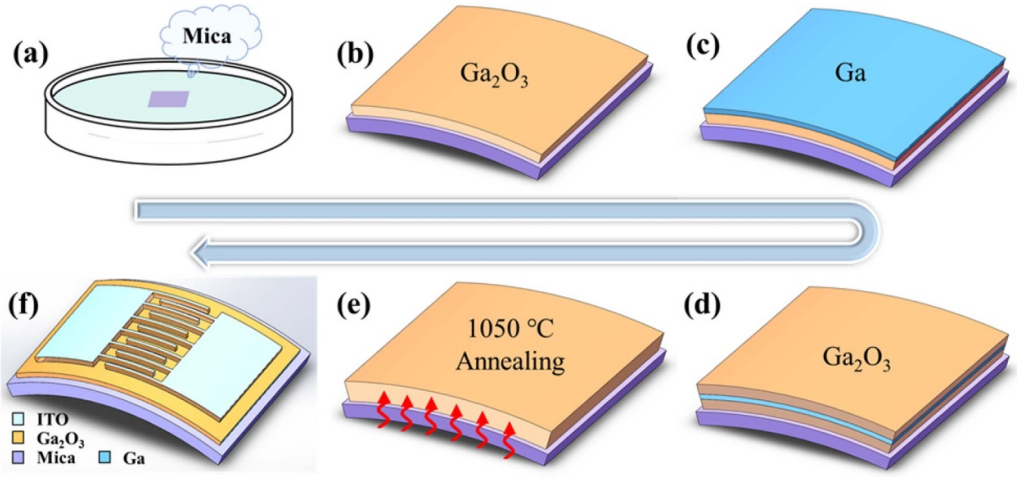

Figure 2. Manufacturing procedure for the β-Ga_2O_3 nanocomposite UV PDs on mica substrates.

2.3. Fabrication of the PDs

The solar-blind UV PDs were fabricated by conventional UV photolithography and lift-off processes. A Sn-doped indium oxide (ITO, 80 nm) layer was sputtered at room temperature to form Schottky contacts with the Ga_2O_3 films [9]. A planar metal-semiconductor-metal (MSM) structure was adopted, with 75 pairs of interdigital fingers configured with a 300 μm length and a 5 μm width, spaced by a 5 μm gap.

2.4. Characterization

An atomic force microscope (AFM, Brucker Multi-Mode 8) and a scanning electron microscope (SEM, Hitachi Regulus 8100) were employed to characterize the surface morphology of the samples. Due to the ultra-low dark current of the PD, a Keithley 4200 semiconductor was used as the source measurement unit to obtain a current–voltage (I–V) curve in the dark. A 254 nm UV irradiation (hand-held lamp) was used as a light source for the I–V curves under illumination and for the time-dependent photoresponse characteristics, and a Keithley 6487 pico-ammeter was used as a power supply. The evaluation of the photoresponse properties in a spectral range from 200 nm to 800 nm was carried out using an Omni-λ 300i (DSR-3110-UV) grating spectrometer. A Raman spectrometer (HR-800) and x-ray diffraction (Malvern Panalytical EMPYREAN SERIES 3) were used to characterize the crystal lattice order and the structures of the thin films.

3. Results and discussions

Figure 1 shows the transmittance and flexibility of bare mica to reveal its advantages as a flexible substrate. Optical images of the mica substrate bent to 30° and 90° are shown in figures 1(a) and (b), respectively. The thickness of a mica substrate with such good flexible performance is generally below 30 μm, such as the one 22 μm thick when measured with a micrometer ruler (the accuracy of this ruler is 1 μm) shown in figure 1(c).

The procedure for preparing a flexible transparent β-Ga_2O_3 solar-blind UV PD on mica is shown in figures 2(a)–(f). First, a mica substrate with a thickness of less than 30 μm was obtained by stripping a mica sheet in the deionized water environment in a petri dish. Secondly, a 60 nm a-Ga_2O_3 film was sputtered on the pretreated mica substrate in a pure argon (Ar) atmosphere with a radio frequency of 60 W at room temperature. Thirdly, a 20 nm metal Ga thin layer was grown on the Ga_2O_3 surface by thermal evaporation. Then another 60 nm a-Ga_2O_3 layer was deposited on the top of the Ga interlayer. The laminated film samples were subsequently annealed at 1050 °C for 30 min to form a β-Ga_2O_3 phase. After that, a UV PD was fabricated by conventional UV photolithography and lift-off processes with a planar MSM structure.

Annealing is an important step in the preparation of the nanocomposite films described in this paper. In order to more intuitively distinguish the effect of annealing on the surface morphology of the films, SEM and AFM characterizations were conducted, as shown in figure 3. Figures 3(a) and (c) show SEM and AFM images of the a-Ga_2O_3/Ga/a-Ga_2O_3 laminated film before annealing, respectively. It can be seen that with the pre-deposited metal Ga layer, dense and uniform crystalline grains are dominant on the surface. It is worth noting that the root mean square (RMS) roughness value was less than 2 nm for the sample without a Ga interlayer [23]. After inserting a thin Ga layer, however, the RMS values increased to 13.78 nm and 25.4 nm before (figure 3(c)) and after annealing (figure 3(d)), respectively. The grains tend to grow and coalesce with an increase of the Ga layer's thickness [10, 11]. Figures 3(b) and (d) show the SEM and AFM images of the a-Ga_2O_3/Ga/a-Ga_2O_3 films after annealing, respectively. Note that the grains on the surface of the annealed sample became sharper with less-rounded edges, compared to those before annealing. In fact, the surface protrusion is composed of the interior discrete metal Ga NSs and the surrounding β-Ga_2O_3 matrix, which has been confirmed by the previous TEM observations [11]. The formation of Ga/Ga_2O_3 nanocomposite films is caused by the migration of Ga atoms

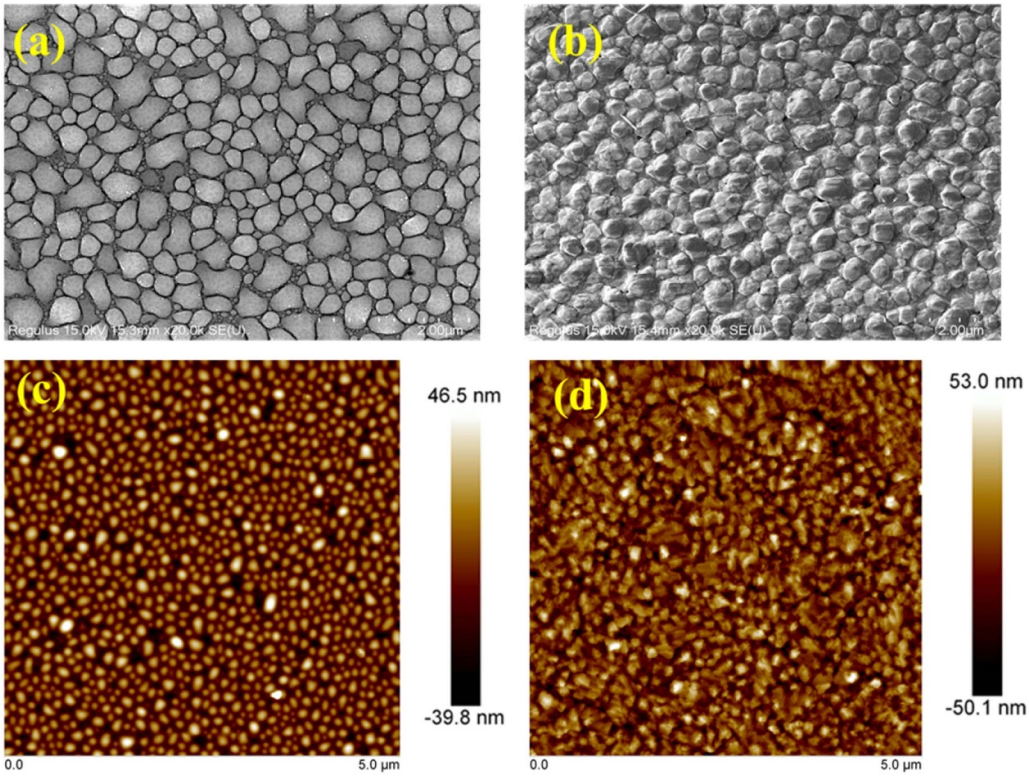

Figure 3. SEM and AFM pictures of the a-Ga_2O_3/Ga/a-Ga_2O_3 films before (a), (c) and after (b), (d) thermal annealing at 1050 °C.

from the interlayer upwards to the surface and their partial oxidation in the thermal annealing process.

According to the XRD curves in figure 4, the annealed β-Ga_2O_3 nanocomposite films have more pronounced diffraction peaks, in good consistency with those of β-Ga_2O_3 (JCPDS Card No. 87–1901) [24]. This result shows that the introduction of a Ga interlayer can help to reduce the defects in β-Ga_2O_3 and form better crystal qualities.

Figure 5 demonstrates the photoresponse performance of the flexible β-Ga_2O_3 solar-blind PD on mica. Figure 5(a) presents the I–V characteristics of the device under a 10 V bias in the dark and under 254 nm illumination by a hand lamp, respectively. It can clearly be seen that the UV PD has a very low dark current (below 10^{-12} A). Such a low background noise can reduce energy consumption and noise interference in practical applications. Meanwhile, the photocurrent can reach more than 10^{-6} A under illumination by 254 nm UV light, indicating a light-to-dark ratio as high as $\sim 3 \times 10^6$. In addition to this remarkable feature, the flexible β-Ga_2O_3 UV PD on mica also illustrates favorable photoresponse repeatability and a relatively fast response performance with no obvious PPC phenomenon (figure 5(b)). Figure 5(c) shows the spectral response characteristics of the PD in a wavelength range of 200 nm to 800 nm. The response peak is located at 250 nm with a sharp cutoff wavelength, which is consistent with previous reports. It should be noted that the rejection ratio of UV (250 nm) to visible light (400 nm) is 6.83×10^3, suggesting the device's potential application as a high-resolution solar-blind UV PD.

In order to further quantify the response speed of the novel flexible transparent β-Ga_2O_3 UV PD on mica, a special circuit was constructed for the measurements. A 10 MΩ load resistor was connected in series with the UV PD, an oscilloscope recorded the bias change of the load resistor and a Keithley 6487 Pico-ammeter was used as a power supply, as shown in figure 6(a). When the device was irradiated with 254 nm UV light, the photo-generated carriers in the β-Ga_2O_3 nanocomposite film caused the resistance of the device to become smaller and thereby the current flowing through the load resistor increased. When the light was removed, the carriers quickly recombined, leading to a reduction in the load current. The oscilloscope connected in parallel with the 10 MΩ load resistor was able to monitor the transient change of voltage across the load resistor, which was a good reflection of the recovery speed of the UV PD. The transient curve obtained by the oscilloscope is shown in figure 6(b). It can be seen that after the 254 nm UV light was turned off, the recovery time (defined as the decrease from 90% to 10% of the initial photocurrent value) was less than 50 ms. Considering the high light-to-dark ratio and the rejection ratio of UV (250 nm) versus visible light (400 nm), this response speed may be beneficial for applications in certain cases.

As mentioned above, compared to commonly used organic plastic substrates, Ga_2O_3 films deposited on mica can endure much higher temperatures, which makes a significant difference to the device's performance. Herein, a flexible a-Ga_2O_3 UV PD was prepared on a Polyethylene naphthalate (PEN) substrate to serve as a contrast to the one on mica, as shown

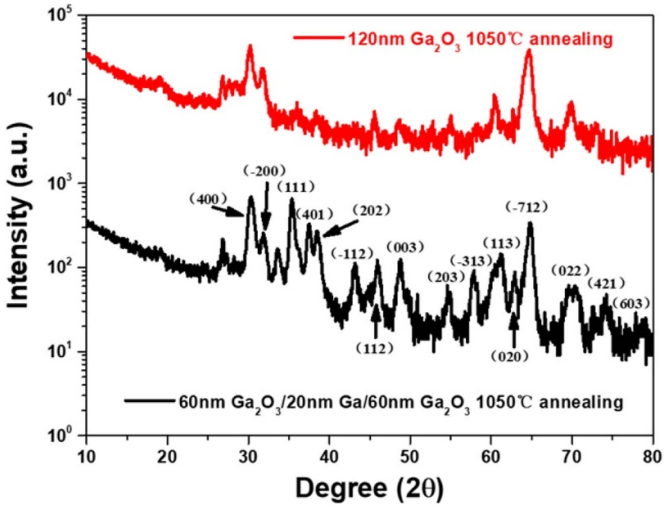

Figure 4. XRD curves of a-Ga_2O_3/Ga/a-Ga_2O_3 after annealing at 1050 °C (black line) and single a-Ga_2O_3 after annealing at 1050 °C (red line). All the labeled peaks correspond to β-Ga_2O_3.

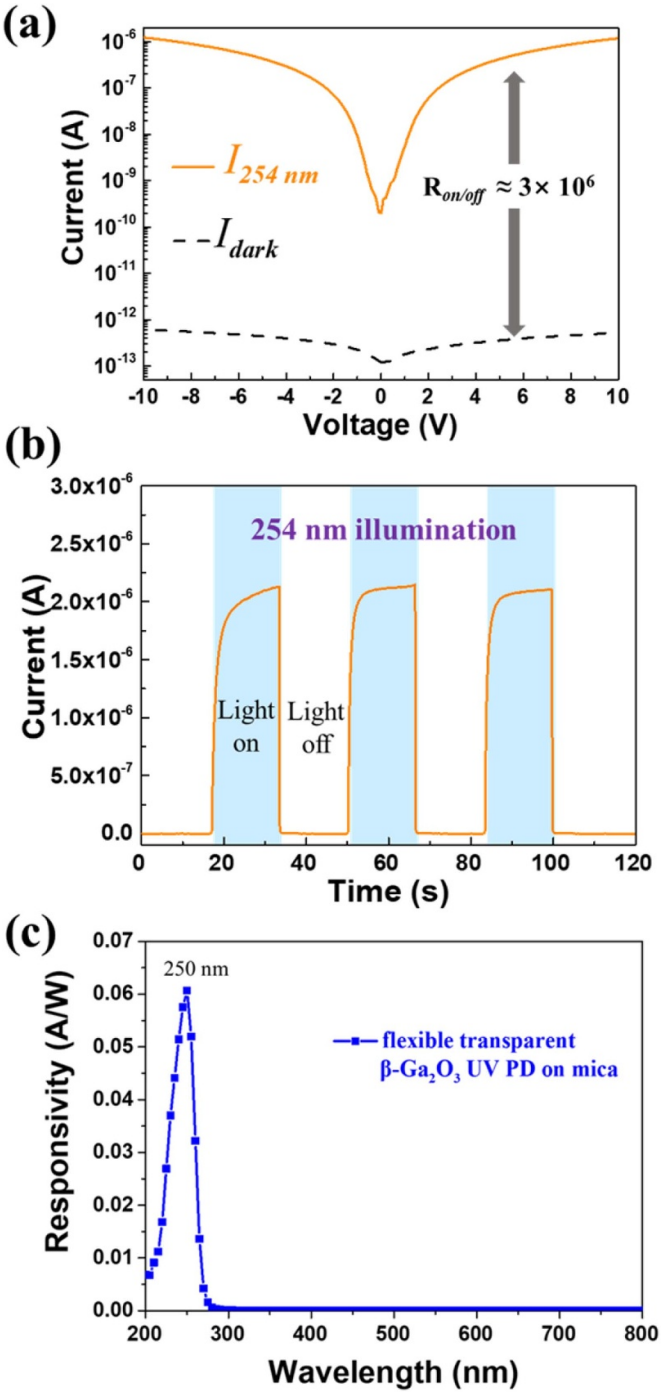

Figure 5. Current-voltage curves in the dark and under 254 nm light illumination (a), time-dependent photocurrent under 254 nm illumination (b), and the responsivity curve (c) of the flexible transparent β-Ga_2O_3 UV PD on mica.

in figure 7. The sputtering conditions of the a-Ga_2O_3 film (120 nm) were the same as for the laminated film on mica. Since the endurance temperature of PEN does not exceed 120 °C, the a-Ga_2O_3 film was grown on PEN at room temperature without any post-annealing process. On the other hand, the flexible β-Ga_2O_3 nanocomposite film on mica was obtained by thermal annealing at 1050 °C. Figure 7(a) presents their I–V curves in the dark and under 254 nm illumination by a hand lamp, respectively. The device on PEN has a high and asymmetric dark current (the black dashed line), which is attributed to the large amount of V_O defects in the a-Ga_2O_3 film grown at room temperature. In contrast, the dark current of the device on mica decreases remarkably, by six orders of magnitude (the blue dashed line). That contributes to a greatly enhanced light-to-dark ratio at a bias voltage of 10 V (>10^6), even though the flexible a-Ga_2O_3 PD on PEN has a larger photocurrent (the black solid line). Another distinction between the two flexible UV PDs is the severe PPC effect and the resulting slow response speed in the a-Ga_2O_3 device on PEN, as shown by the black line in figure 7(b). Therefore, high-temperature processing can greatly improve the response speed and light-to-dark ratio of the device. Mica substrates that can withstand high temperatures have great potential for use in flexible and transparent optoelectronics, leading to a fewer temperature limitations for the preparation of flexible devices.

A comparison of the photoresponse parameters of the flexible β-Ga_2O_3 nanocomposite PD on mica as described in this work and the other previously reported Ga_2O_3-based devices is listed in table 1. Our fully transparent and flexible β-Ga_2O_3 PD shows a relatively larger I_{photo}/I_{dark} ratio and a larger UV (250 nm) to visible light (400 nm) rejection ratio, as well as a comparable decay time under a compatible incident power density.

Enhanced photoresponse properties due to the surface plasmon resonant effect have been demonstrated in our previous reports [10, 11]. On the other hand, high-temperature post annealing is generally supposed to give rise to a significant reduction of defects in the annealed samples. To explore the effect of the Ga interlayer in the Ga_2O_3/Ga/Ga_2O_3 structure on repairing the lattice, Raman spectroscopy measurements were applied to the 1050 °C annealed samples of M1, M2, Q1, and Q2 (figure 8). The excitation light source was 325 nm. It can be clearly seen that M2 and Q2, the films with a Ga interlayer, have more and sharper Raman peaks

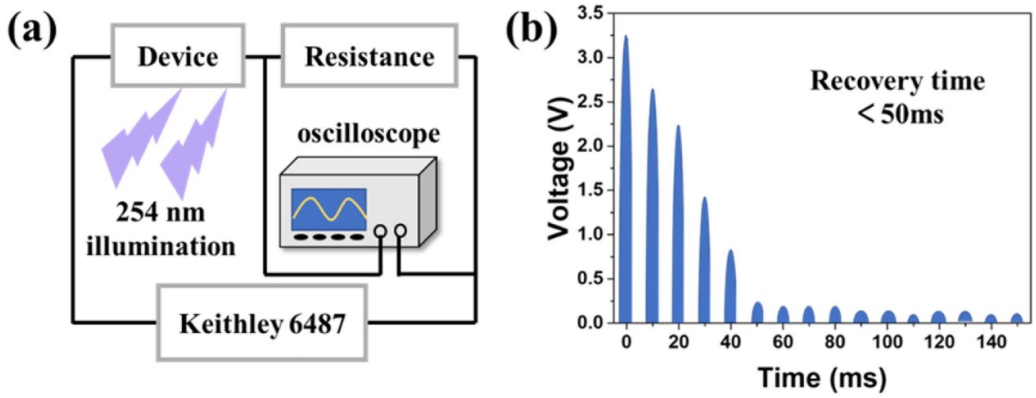

Figure 6. A schematic diagram of the electrical circuit (a) and the transient voltage curve recorded by the oscilloscope (b) in the recovery speed test.

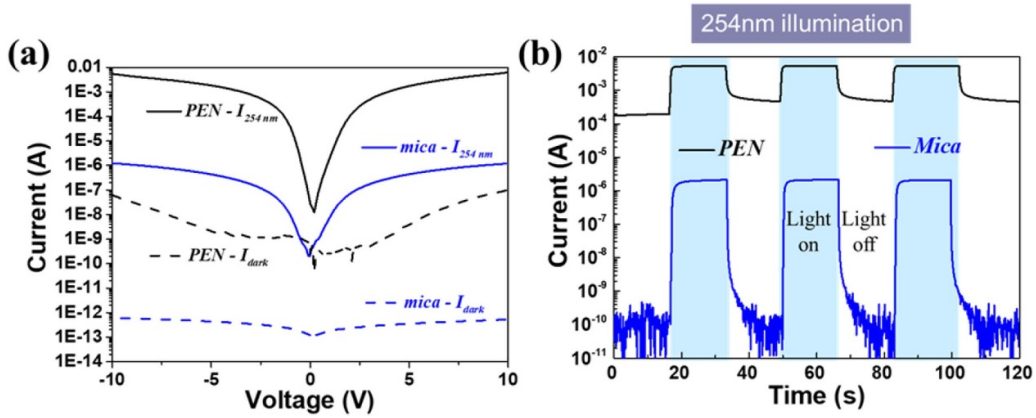

Figure 7. The current-voltage curves in the dark and under 254 nm light illumination (a), and the time-dependent photocurrent under 254 nm illumination (b) for the flexible transparent Ga_2O_3 UV PDs on mica and PEN, respectively.

Table 1. Comparison of the photoresponse parameters of the flexible β-Ga_2O_3 nanocomposite PD on mica in this work and the other previously reported devices ('–' means not mentioned or not clear in the literature).

Material	Rejection ratio	Decay time	I_{photo}/I_{dark} ratio	Flexible/transparent	Incident power density	Ref.
β-Ga_2O_3 thin film	$>1 \times 10^3$	78 ms	$>1 \times 10^3$	no/no	–	[25]
a-Ga_2O_3 thin film	$>1 \times 10^5$	~0.1 s	$>1 \times 10^3$	no/no	70.5 μW cm^{-2}@254 nm	[26]
a-Ga_2O_3 thin film	2.7×10^4	380 ms	$>1 \times 10^5$	yes/yes	200 μW cm^{-2}@254 nm	[27]
a-(GaO_X) film	558	148 μs	$\sim 1 \times 10^4$	no/yes	700 μW cm^{-2}@253 nm	[28]
a-Ga_2O_3 thin film	$>10^4$	19.1/80.7 μs	$>10^4$	no/yes	20 μW cm^{-2}@254 nm	[10]
a-(Mg:GaOx) film	–	0.15 s	338	no/no	17.6 μW cm^{-2}@255 nm	[29]
3D a-Ga_2O_3 thin film	$>10^2$	0.308/1.7 ms	$>10^4$	yes/yes	1.11×10^4 μW cm^{-2}@266 nm	[30]
β-Ga_2O_3 nanocomposite film	–	–	8.05×10^5	no/yes	20 μW cm^{-2}@254 nm	[9]
β-Ga_2O_3 nanocomposite film	6.83×10^3	<50 ms	3×10^6	yes/yes	20 μW cm^{-2}@254 nm	This Work

than M1 and Q1 (the films without the Ga interlayer), mostly appearing in the range of 400 ~ 750 cm^{-1}. The Raman peaks at 199 cm^{-1}, 316 cm^{-1}, 345 cm^{-1}, 416 cm^{-1}, 473 cm^{-1}, 629 cm^{-1}, 653 cm^{-1} and 765 cm^{-1} correspond to the crystalline peaks of β-phase Ga_2O_3, mainly due to the bending vibration mode of the $Ga_I(O_I)_2$ octahedron and the Ga_IO_4 stretching

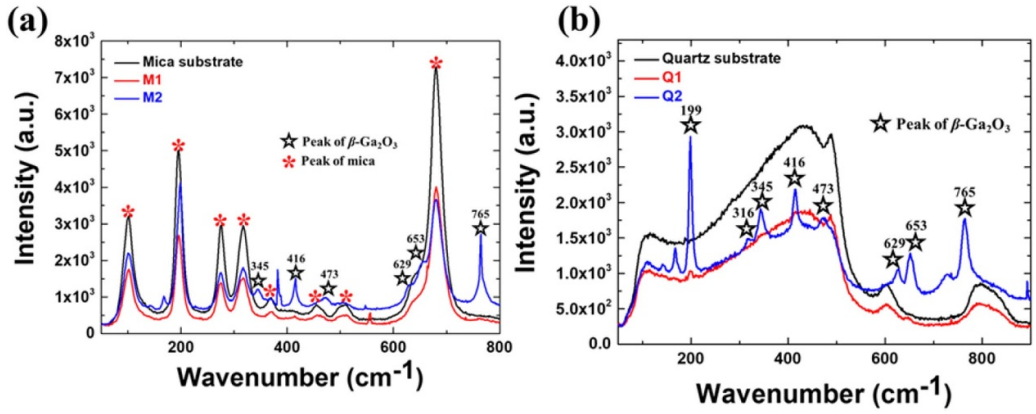

Figure 8. Raman spectra of the 1050 °C-annealed Ga_2O_3 single-layer films and Ga_2O_3 laminated films on mica (a) and quartz (b) substrates.

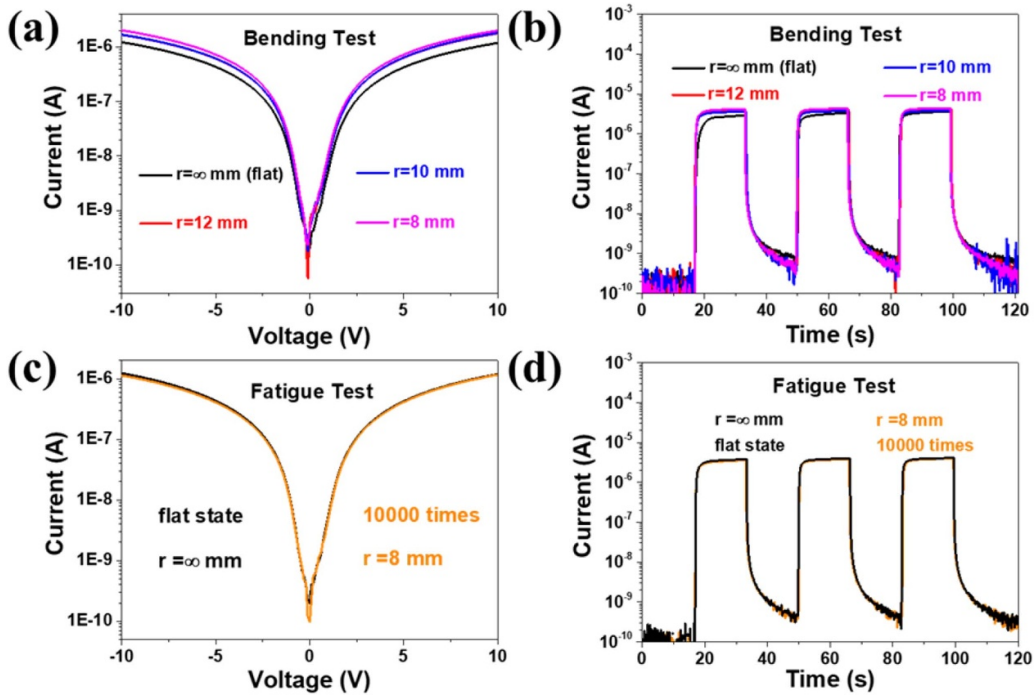

Figure 9. Bending tests for $r = \infty$ mm, 8 mm, 10 mm, 12 mm and the 10 000 cycle fatigue test ($r = 8$ mm) of the solar-blind UV PD based on the 1050 °C-annealed β-Ga_2O_3 film on mica.

and bending vibration modes [31, 32]. The enhancement of the two vibration modes in the annealed β-Ga_2O_3 nanocomposite films is ascribed to the more stoichiometric and ordered lattice. We speculate that the diffusion of Ga atoms at high temperatures leads to better crystallinity and fewer defects in β-Ga_2O_3. Further investigations are needed to clarify this issue.

To investigate the effects of the bending state on the photoresponse characteristics of the flexible β-Ga_2O_3 solar-blind UV PDs, photocurrent-voltage curves, temporal response and fatigue measurements were obtained under different bending conditions. A diagrammatic sketch of the flexible device undergoing a bending test is shown in figure 2(f). The curved device is thought to be located on a circumference with a radius r, whose value represents the degree of curvature. Figure 9(a) shows the photocurrent-voltage curves while exposed to 254 nm UV irradiation under the bending radii of 12 mm, 10 mm, and 8 mm, respectively. The temporal photoresponse performance of the device with the same bending radius, r, is displayed in figure 9(b). As shown in figures 9(a) and (b), the flexible β-Ga_2O_3 solar-blind UV PD on mica exhibits almost the same behavior in its bent states as as in the flat state, with negligible influence due to bending stress, suggesting satisfying flexibility. The ignorable difference in these curves may be ascribed to the different contact conditions between the wire and the electrodes when the devices are bent. Figures 9(c) and (d) show the photocurrent—voltage curves and the temporal photoresponse performance while exposed to 254 nm UV light after being mechanically

bent for 10 000 cycles at a curvature degree $r = 8$ mm. The fatigue test presents almost the same curves, even after 10 000 bending cycles. This indicates that flexible β-Ga_2O_3 PD on mica has gratifying robustness and promising applications in the flexible and transparent photoelectric areas.

4. Conclusions

In summary, we have fabricated flexible β-Ga_2O_3 solar-blind UV PDs on a mica substrate by using a post-annealing process. The device's performance is dramatically improved, compared to PDs made on the common flexible substrate, as evidenced by an extremely low dark current of 0.6 pA at a 10 V bias, a very high light-to-dark ratio of 3×10^6, a fast recovery speed of <50 ms, and nearly no degradation under different bending conditions and after a 10 000 cycle fatigue test. The insertion of a gallium interlayer and treatment by high-temperature post annealing are proposed to contribute to the better stoichiometry and lattice order of the β-Ga_2O_3 thin film, which benefits the promotion of photodetection capabilities. This work reveals the remarkable and practical advantages of flexible mica substrates in high-temperature technology and provides a significant reference for boosting the performance of flexible and transparent optoelectronics in extreme environments.

Acknowledgments

This work was supported by the National Natural Science Foundation of China (Grants No. 11675280, 11674405, 61874139, 11875088, and 61904201).

ORCID iDs

Wenxing Huo https://orcid.org/0000-0002-1832-9328
Zengxia Mei https://orcid.org/0000-0002-2034-659X

References

[1] Li D, Jiang K, Sun X and Guo C 2018 AlGaN photonics: recent advances in materials and ultraviolet devices *Adv. Opt. Photon.* **10** 43–110
[2] Du X, Mei Z, Liu Z, Guo Y, Zhang T, Hou Y, Zhang Z, Xue Q and Kuznestov A 2009 Controlled growth of high-quality ZnO-based films and fabrication of visible-blind and solar-blind ultra-violet detectors *Adv. Mater.* **21** 4625
[3] Hou Y, Mei Z and Du X 2014 Semiconductor ultraviolet photodetectors based on ZnO and $Mg_xZn_{1-x}O$ *J. Phys. D: Appl. Phys.* **47** 283001
[4] Chen X, Ren F, Gu S and Ye J 2019 Review of gallium-oxide-based solar-blind ultraviolet photodetectors *Photon. Res.* **7** 381–415
[5] Chen X, Ren F, Ye J and Gu S 2020 Gallium oxide-based solar-blind ultraviolet photodetectors *Semicond. Sci. Technol.* **35** 023001
[6] Chen Y, Lu Y, Lin C, Tian Y, Gao C, Dong L and Shan X 2018 Self-powered diamond/β-Ga2O3 photodetectors for solar-blind imaging *J. Mater. Chem.* C **6** 5727–32
[7] Orita M, Ohta H, Hirano M and Hosono H 2000 Deep-ultraviolet transparent conductive β-Ga_2O_3 thin films *Appl. Phys. Lett.* **77** 25
[8] Sang L, Liao M and Sumiya M 2013 A comprehensive review of semiconductor ultraviolet photodetectors: from thin film to one-dimensional nanostructures *Sensors* **13** 10482–518
[9] Cui S, Mei Z, Zhang Y, Liang H and Du X 2017 Room-temperature fabricated amorphous Ga_2O_3 high-response-speed solar-blind photodetector on rigid and flexible substrates *Adv. Opt. Mater.* **5** 1700454
[10] Cui S, Mei Z, Hou Y, Chen Q, Liang H, Zhang Y, Huo W and Du X 2018 Enhanced photoresponse performance in Ga/Ga_2O_3 nanocomposite solar-blind ultraviolet photodetectors *Chin. Phys.* B **27** 067301
[11] Cui S, Mei Z, Hou Y, Sun M, Chen Q, Liang H, Zhang Y, Bai X and Du X 2018 Surface plasmon enhanced solar-blind photoresponse of Ga_2O_3 film with Ga nanospheres *Sci. China Phys. Mech. Astron.* **61** 107021
[12] Han Z, Liang H, Huo W, Zhu X, Du X and Mei Z 2020 Boosted UV photodetection performance in chemically etched amorphous Ga_2O_3 thin-film transistors *Adv. Opt. Mater.* **8** 1901833
[13] Kumar N, Arora K and Kumar M 2019 High performance, flexible and room temperature grown amorphous Ga_2O_3 solar-blind photodetector with amorphous indium-zinc-oxide transparent conducting electrodes *J. Phys. D: Appl. Phys.* **52** 335103
[14] Zhang Y, Chen X, Xu Y, Ren F, Gu S, Zhang R, Zheng Y and Ye J 2019 Transition of photoconductive and photovoltaic operation modes in amorphous Ga_2O_3-based solar-blind detectors tuned by oxygen vacancies *Chin. Phys.* B **28** 028501
[15] Chang K and Wu J 2005 Formation of β-Ga_2O_3-TiO_2 'Nanobarcodes' from core-shell nanowires *Adv. Mater.* **17** 241–5
[16] Guo D *et al* 2014 Fabrication of β-Ga_2O_3 thin films and solar-blind photodetectors by laser MBE technology *Opt. Mater. Express* **4** 1067–76
[17] Lany S and Zunger A 2007 Dopability, intrinsic conductivity, and nonstoichiometry of transparent conducting oxides *Phys. Rev. Lett.* **98** 045501
[18] Liu X, Guo P, Sheng T, Qian L, Zhang W and Li Y 2016 β-Ga_2O_3 thin films on sapphire pre-seeded by homo-self-templated buffer layer for solar-blind UV photodetector *Opt. Mater.* **51** 203
[19] Peng H, Dang W, Cao J, Chen Y, Wu D, Zheng W, Li H, Shen Z and Liu Z 2012 Topological insulator nanostructures for near-infrared transparent flexible electrode *Nat. Chem.* **4** 281–6
[20] Chu Y 2017 Van der Waals oxide heteroepitaxy *Npj Quantum Mater.* **5** 67
[21] Yang Y, Gao W, Xie Z, Wang Y, Yuan G and Liu J 2018 An all-inorganic, transparent, flexible, and nonvolatile resistive memory *Adv. Electron. Mater.* **4** 1800412
[22] Bitla Y and Chu Y 2017 MICAtronics: a new platform for flexible X-tronics *FlatChem* **3** 26–42
[23] Sui Y, Liang H, Chen Q, Huo W, Du X and Mei Z 2020 Room-temperature ozone sensing capability of IGZO-decorated amorphous Ga_2O_3 films *ACS Appl. Mater. Interfaces* **12** 8929–34
[24] Geller S 1960 Crystal structure of β-Ga_2O_3 *J. Chem. Phys.* **33** 676
[25] Arora K, Goel N, Kumar M and Kumar M 2018 Ultrahigh performance of self-powered β-Ga_2O_3 thin film solar-blind

photodetector grown on cost-effective Si substrate using high-temperature seed layer *ACS Photon.* **5** 2391–401

[26] Qian L, Wu Z, Zhang Y, Lai P, Liu X and Li Y 2017 Ultrahigh-responsivity, rapid-recovery, solar-blind photodetector based on highly nonstoichiometric amorphous gallium oxide *ACS Photon.* **4** 2203–11

[27] Li Z *et al* 2019 Flexible solar-blind Ga_2O_3 ultraviolet photodetectors with high responsivity and photo-to-dark current ratio *IEEE Photon. J.* **11** 6803708

[28] Lee S, Kim S, Moon Y, Kim S, Jung H, Seo M, Lee K, Kim S and Lee S 2017 High-responsivity deep-ultraviolet-selective photodetectors using ultrathin gallium oxide films *ACS Photon.* **4** 2937–43

[29] Zhang D, Du Z, Ma M, Zheng W, Liu S and Huang F 2019 Enhanced performance of solar-blind ultraviolet photodetector based on Mg-doped amorphous gallium oxide film *Vacuum* **159** 204–8

[30] Chen Y, Lu Y, Liao M, Tian Y, Liu Q, Gao C, Yang X and Shan C 2019 3D solar-blind Ga2O3 photodetector array realized via origami method *Adv. Funct. Mater.* **8** 1906040

[31] Dohy D and Lucazeau G 1982 Raman spectra and valence force field of single-crystalline β-Ga_2O_3 *J. Solid State Chem.* **45** 180–92

[32] Hou Y, Wu L, Wang X, Ding Z, Li Z and Fu X 2007 Photocatalytic performance of α-, β-, and γ-Ga2O3 for the destruction of volatile aromatic pollutants in air *J. Catal.* **250** 12–18